2024 IEEE/RSJ International Conference on Intelligent Robots and Systems (IROS)
October 14-18, 2024. Abu Dhabi, UAE

Parametric Synthesis of Compliant Joints for Impact-Robust Shaftless Leg Mechanisms

Egor A. Rakshin[1], Dmitriy V. Ogureckiy[1], Ivan I. Borisov[1,2], and Sergey A. Kolyubin[1]

***Abstract*— This paper describes a novel parametric optimization procedure for three flexure cross hinges (TFCH) integrated into multi-link leg mechanisms with closed-loop kinematics. Despite advantages such as compliance, no need for joint lubrication, light weight and cost-efficiency, such shaftless mechanisms have not been widely used, especially in the field of dynamic locomotion, also because their design is challenging and barely studied. Using a morphological computation approach, we have optimized the TFCH geometry to achieve the desired joint stiffness using frequency analysis, ensuring safe and stable hopping under external perturbations. We combined rigid body dynamics with lumped stiffness model and finite element modeling using the SPACAR toolbox to simulate various designs within our optimization pipeline. To illustrate the efficiency of the resulting designs, we built a prototype and conducted a series of full-scale experiments with ramp jumps whose trajectories were recorded by a motion capture system. The experiments showed that TFCH can be effectively integrated into leg mechanisms, providing benefits such as impact robustness, energy recuperation, and the ability to work in extreme conditions.**

I. Introduction

Robots require fast motions, forceful contacts, impacts mitigation, compliance with safety requirements, etc. Meeting these requirements should not affect the robot's ability to move dynamically in a complex environment with unpredictable interaction with physical objects. Robot's hardware and software have to prevent from damaging the robot itself, surrounding environment, and humans. To ensure the safety and reliability of robots when working in unstructured environments, the passivity property must be taken into account [1].

Passivity can be implemented at either the software or physical level. Software solutions such as impedance control, while proven to be robust and effective, necessitate accurate position and force sensors to control a robot's state and simulate passivity [3]. Passivity can be achieved at the physical level using elastic elements. The physical properties of an elastic or flexible element allow it to store potential energy when deformed. This enables it to amplify the generated power and make use of low-power actuators. Furthermore, it can release the stored energy in a powerful burst and has an unlimited bandwidth [4].

*This work was supported by the Analytical Center for the Government of the Russian Federation (IGK 000000D730321P5Q0002), agreement No. 70-2021-00141.

[1]Egor A. Rakshin, Dmitriy V. Ogureckiy, Ivan I. Borisov, and Sergey A. Kolyubin are with the Biomechatronics and Energy-Efficient Robotics (BE2R) Lab, ITMO University, Saint Petersburg, Russia e-mail: {earakshin, s.kolyubin}@itmo.ru

[2] Ivan I. Borisov is also with the SberRoboticsCenter, Moscow, Russia

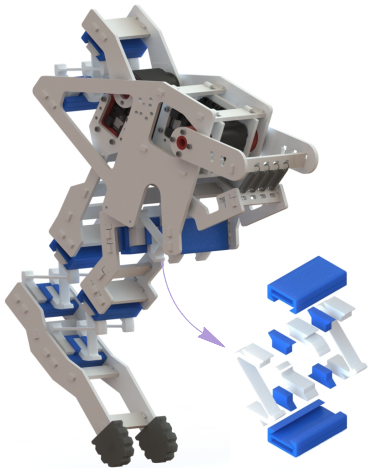

Fig. 1. CAD render of a hopping robot from [2] but equipped with elastic joints only, i.e. TFCH, for impact robustness, energy recuperation, and torque peak mitigation

This paper presents a co-design method to solve the elasticity allocation problem for a linkage mechanism with closed kinematics. We believe that our method is versatile enough to be employed in the synthesis of various types of robots. Nonetheless, in the context of this study, we have chosen to apply the proposed method specifically to the synthesis of a hopping robot. This choice has been made in order to validate the efficacy and effectiveness of our approach.

To provide the required stiffness, the elastic elements can be combined into a compliant joint (CJ) and there are various solutions for shaping the geometrical parameters and topology of CJs [5]. In this study we utilize CJs to replace rotational bearings, adapt to external forces, eliminate backlash, get rid of lubrication, get the desired stiffness while maintaining geometric and stress constraints [6]. To verify the feasibility of the proposed method, we built a prototype of a hopping robot equipped with CJs in constrained joints (Fig. 1), replacing conventional bearings.

A. Related Work

Flexible links and CJs can be used as a source of compliance to compensate robot weight [7]; to withstand high dynamic loads during touchdown phase of locomotion [8], [9]; to use elastic components as a passive source of torques [10]. Series elastic actuators (SEA) [11] can be used for resonance-based locomotion tasks [12], and parallel elastic actuators (PEA) with drive couplings are capable of storing energy, recovering it in a single explosive impact [13].

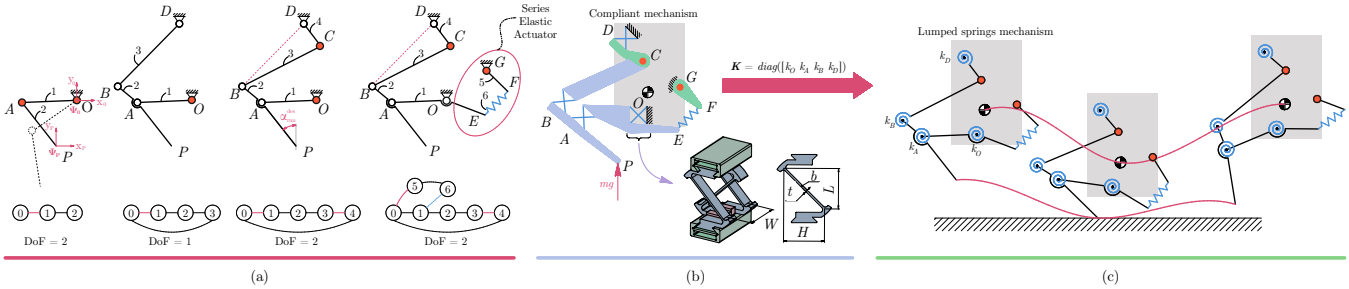

Fig. 2. The proposed design: (a) mechanism and (b) compliant joints synthesis, (c) motion trajectory planning and control

When the shape, geometry, and arrangement of elastic bodies in CJs are unknown, topology optimization algorithms can be applied. The goal is to determine the most efficient structure that satisfies given criteria, such as desired rotational and longitudinal stiffnesses [14], uniform stress distribution across all deformable bodies [15], or the highest strain energy density [16].

The biggest disadvantage of topology optimization is that the method is computationally expensive and does not ensure convergence. A method of structural-parametric synthesis of flexible joints with desired stiffness and precise motion based on modular "building" blocks is given in [17]. The topologies of the blocks are specified, so the optimization problem is reduced to finding the best combination of these blocks and their geometry.

B. Contribution & Overview

CJs must be able to handle large deformations and distributed stresses, have minimal displacement of the center of rotation, and have enough stiffness in the longitudinal direction to avoid collapsing under load, CJs should be easily fabricated using additive manufacturing techniques for rapid prototyping and have minimal subsequent machining. The three flexure cross hinge topology (TFCH) fulfills these requirements [6].

Within this paper, only TFCH is considered for the sake of brevity and to verify the proposed method. In the context of this work, the main goal is to improve robot adaptability and potentially energy efficiency. Consequently, we introduce the novel contribution of this paper: a design method for dynamically locomotive robots with compliant joints, demonstrated through the following statements:

- The co-design method to solve the *elasticity allocation problem* for a linkage mechanism with closed kinematics under dynamic forceful interaction
- The three flexure cross hinge topology (TFCH) can be used to provide *safe interaction* with unstructured environment and *energy efficiency* through potential energy recuperation.

The rest of the paper is organized as follows: the following section II describes our proposed pipeline in detail. The III section presents a description of the prototype we developed and the physical experiment we conducted. Conclusions and suggestions for future work are presented in the IV section.

II. Proposed Method Outline

The design procedure consists of several steps (Fig. 2): (1) synthesis of the mechanism, i.e., optimization of the topology and linkage geometry, (2) CJ allocation involving finite element modeling (FEM), (3) motion planning and actuator control, and (4) final prototyping to verify the obtained results. We call the problem of finding the optimal configuration of flexible joints and their stiffness *the stiffness allocation problem*.

CJs do not operate as an ideal rotational joint due to the parasitic center of rotation displacement during deformation. Nevertheless, a simplified model of a closed chain leg with rigid joints was used in the dynamics simulation for faster modeling without calculating large deflections of elastic bodies. We have used MATLAB Simscape Multibody as the simulation modeling tool.

Since CJs cannot perform unbounded rotation, we need closed-loop kinematics to limit the possible rotation angles. This paper focuses on the synthesis of CJs rather than topological optimization of closed-loop chain kinematics. Thus, we used the previously proposed method to optimize the links geometric parameters, mass and elasticity distribution for a closed-loop leg mechanism of a hopping robot [2].

The SPACAR toolbox for MATLAB environment was chosen for modeling elastic joints because it allows high-fidelity modeling, calculates the resonant frequencies of the entire compliant mechanism [18], and requires less computational resources compared to CAE systems.

We applied global non-gradient optimization for CJs geometry synthesis and motors trajectory planning. Due to nonconvex objective function, we used genetic algorithm from Global Optimization Toolbox.

The pipeline can be used to create mechanisms for grasping, wearable rehabilitation devices, exoskeletons, robot arms and legs, and other closed kinematics linkage mechanisms.

For the hopping robot, we consider only two dynamic motions: jumping on a place and forward hopping. To simplify the task of motion planning, we use parametric sine wave as a position references for motors. With the two sine waves, we can manipulate the signal parameters to obtain the necessary trajectory to perform the desired dynamic behavior.

A. Rigid-body closed-chain mechanism synthesis

1) Topology of the basic mechanism: The topology of the leg with closed chain kinematics and optimization procedure was taken from our previous study [2]: the five-bar mechanism with two degrees of freedom (DoF). The five-bar mechanism is structurally the simplest topology of closed chain kinematics with two degrees of freedom, and besides we can compare the modification with the previous result. This subsection relies on contribution of [2].

According to the Chebychev–Grübler–Kutzbach criterion, DoF of a planar mechanism can be calculated as:

$$W = 3N - 2p \tag{1}$$

where W is number of DoF, N is a number of moving links, and p is a number of lower kinematic pairs such as revolute or prismatic joints.

If we extract p for $W = 2$, we get the following:

$$p = \frac{3}{2}N - 1,\ p \in \mathbb{Z}, \tag{2}$$

where N has to be an even number. If we exclude the pair $[N,\ p]$ = [2, 2] since it is an open chain mechanism, the smallest number set we can get is $[N,\ p]$ = [4, 5], which means a five-bar closed chain mechanism.

The parametric synthesis of link lengths was performed such that one motor performs sinusoidal wave motion (main motor) and the second motor (mode motor) is designed to act as a source of reconfiguration of the mechanism by changing the contact point trajectory.

Despite the presence of CJs capable of partially dampening shock loads, SEA was added to the main motor. This choice is justified because the CJs with high longitudinal stiffness do not guarantee complete external shocks decoupling from the motor and increase backdrivability [19].

2) Desired trajectory: The task is to get the desired angle of attack α (Fig. 2, a) and then obtain the initial angles of the passive revolute joints $[O,\ A,\ B,\ D]$ where CJs have to be placed.

For the chosen mechanism topology and link lengths, the feasible smallest angle of attack for jumping is $\alpha_{run}^{des} = 75^\circ$. To obtain the desired trajectory it is necessary to solve the forward kinematics (FK) problem in the form of

$$q_d = f(q_i), \tag{3}$$

where dependent and independent coordinates q_d, q_i form the holonomic constraints $N_c = 0$.

Firstly FK was simplified to a four bar mechanism by fixing link BD and using trigonometric transformations (Fig. 2, a). Then, links DC and CB were included. To calculate the actual angle of attack for the jump motion α_{run}^{act}, the inverse kinematics (IK) problem must be solved. To simplify the calculation we reduce IK to the following optimization problem:

$$\min_{q_i^{act}} \quad \left(P(q_i^{des}) - P(q_i^{act})\right)^2, \tag{4}$$

where P is a toe position vector in frame Ψ_P related with inertial frame Ψ_O.

B. Compliant mechanism co-design

In this step, we focus on integrating CJs as components of a compliant mechanism, optimizing resonant frequencies, and developing effective motion planning strategies with lumped stiffnesses.

1) Compliant mechanism: Parameters of the TFCH with two symmetric side (s) leafsprings and one central (c) are

$$\begin{aligned} P^{TFCH} &= [L_c,\ L_s,\ H_c,\ H_s,\ t_c,\ t_s,\ b_c,\ b_c,\ W] \\ \mathbf{A}P^{TFCH} &< \mathbf{b} \\ t_{c,s} &= 0.4n, n \in \mathbb{Z}, \end{aligned} \tag{5}$$

where L, H, t, b, W are the leaf spring length, height, thickness, width, and hinge width, respectively, in the undeformed state (see Fig. 2, b for an illustration of the geometrical parameters of the TFCH).

To constrain the size of the hinge and to ensure that the springs have clearances so that they do not interfere with each other, we introduce a linear inequality, where $\mathbf{A}$ and $\mathbf{b}$ are the constraint matrix and vector, respectively. Since we produce CJ using FDM 3D printing and the nozzle has a fixed diameter of 0.4 mm, we constrain the thickness using integer constraints.

Since the mechanism has four CJs $[O,\ A,\ B,\ D]$, total optimization vector of the mechanism is

$$P^{mech} = \underbrace{[P_O^{TFCH},\ P_A^{TFCH},\ P_B^{TFCH},\ P_D^{TFCH}]}_{36\times 1}. \tag{6}$$

2) Joints synthesis: To operate on compliance of the mechanism, we can use stiffnesses of the CJs (Fig. 2, b). However, this approach is impractical because the CJs motion is not circular and obtaining only the rotational stiffness would be incorrect. Another method is to obtain the resonant frequency of the entire mechanism by solving the eigenvalue problem [6]. This yields a list of mode shapes, in which the smallest one is the frequency of leg motion of interest. The task is to bring the frequency to the desired value. CJs that are too stiff result in a "statue" mechanism where the motors cannot move the links. On the other hand, CJs that are too weak cannot support the weight of the robot and collapse after a touchdown.

The movement of the flexible leg is influenced by the stiffness of its joints, which are limited in their range of rotation due to yield constraints. For the TFCH topology, the limiting range of motion was chosen between -45° and 45° [17]. To objectify the frequency selection, we first analyze the maximum joint motion and adjust the frequency so that it satisfies the constraint criteria. Since impact force depends on a contact model, for the sake of simplicity, we applied a static force equivalent to the robot weight $m = 0.5$ kg with multiplication factor of 2 for a model loaded in SPACAR. By applying this load, we set the strain and stress limits to obtain the operating ranges of the CJs.

The procedure of the optimization is shown at Fig. 3. During initialization, we set the robot geometry, initial parameters, and optimization constraints.

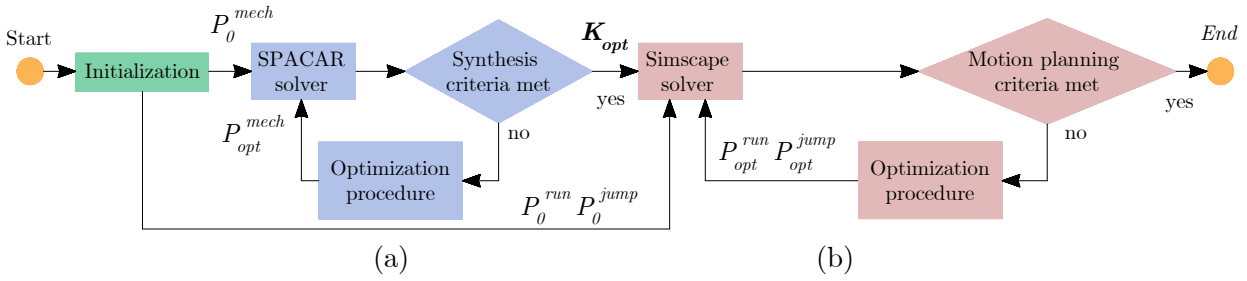

Fig. 3. Optimization procedure: (a) CJs synthesis and stiffness matrix **K** extraction, (b) motors motion planning for jumping and hopping behavior

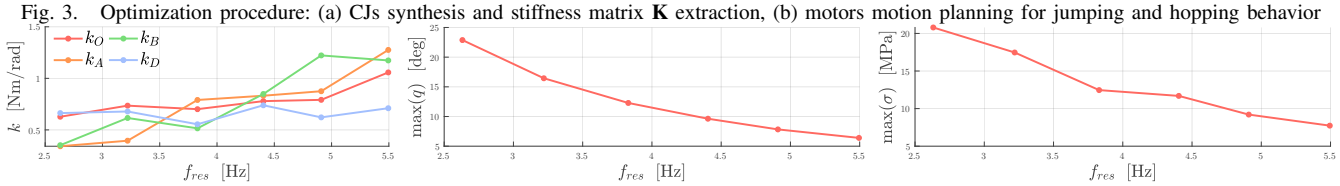

Fig. 4. The relationship between stiffness, strain, and stress on frequency

SPACAR calculates the stiffness matrix **K** from given parameters vector P^{mech}. The synthesis criteria are:

$$\begin{cases} \min\limits_{P^{mech}} & -f^{leg}(P^{mech}), \\ s.t. & \sigma^{max} \leq [\sigma], \\ & q^{CJ} \in [\max(q^{des}) \pm q^{soft}], \end{cases} \tag{7}$$

where f^{leg} is the frequency of a mode shape of interest, σ^{max}, $[\sigma]$ are the maximum stress and yield stress respectively, q^{CJ}, $max(q^{des})$, and q^{soft} are current deflection of CJ, maximum deflection, and soft constraint respectively. Results of synthesis procedures are shown in Fig. 4. A frequency of 2.63 Hz was chosen since it ensures large deflection under desired motion range.

3) Motion planning: On the next step the stiffnesses are transferred to the motion planning procedure (Fig. 3). Here, the mechanism with lumped springs (Fig. 2, *c*) is modeled in MATLAB Simscape Multibody. Since the toe position (contact point) is known through the FK problem, we can create a motor control sequence. This paper examines the use of simple constant and sinusoidal reference position control, as opposed to utilizing complex control algorithms and motion planning strategies. When moving, the angles of the motors change in a sinusoidal pattern. However, for jumping, the reference motor angle remains constant. The mode motor temporarily fixes the leg, providing the desired angle of attack, while the main motor with SEA performs the jumping movements.

The parameter vectors to be tuned for running and jumping behaviors are the following:

$$\begin{aligned} P^{run} &= [A_{main}, A_{mode}, F_{main}, F_{mode}, B_{main}, B_{mode}, \varphi_{mode}], \\ P^{jump} &= [A_{main}, F_{main}, B_{main}, C_{mode}], \end{aligned} \tag{8}$$

where A, F, B, φ, and C are amplitude, frequency, bias, phase shift of sine waves, and constant value respectively.

Objectives for the running and jumping behaviors:

$$\begin{aligned} &\min_{P^{run}} -\frac{X_{end}\tilde{V}}{E_{end}}, \\ &\min_{P^{jump}} -\tilde{h}, \end{aligned} \tag{9}$$

where X_{end}, $\tilde{V}$, E_{end}, $\tilde{h}$ are the total distance traveled, mean longitudinal speed, total energy consumed, and mean jumping height respectively.

III. Design

A. Physical prototype

A physical prototype was fabricated to verify the proposed co-design method (Fig. 5, *a*). We used a laser cutter to facilitate the assembly processes and fabrication of body parts from polyoxymethylene (POM) sheets. 3D printers were used to fabricate the guides and CJs from PETG and PA6 nylon, respectively. The choice of nylon is justified by good mechanical properties of this polymer under elastic deformations. The body parts were connected to each other using hooks and fastening clips. The components of the CJs are manufactured as prismatic parts without the need for additional supports. This design decision was made due to the challenges of printing nylon supports and the potential for damaging the CJs when removing them. The CJs' parts are fixed via dovetail guides and are held in place by frictional forces. The total mass of the robot is 530 grams. A toe (contact point) is made of rubber-like TPU A95 plastic to increase surface adhesion. Steel and other elastic metals possess thinner hysteresis regions, leading to lower material damping compared to nylon. This translates into enhanced energy preservation capabilities. Since this study is at the prototype level, nylon was chosen as a polymer that is more convenient in terms of rapid prototyping and availability.

We used Dynamixel AX-18A as actuators because of their availability and good power characteristics. The motors are controlled using *Arduino Nano Every* and a *74LVC2G241* interface converter for communication.

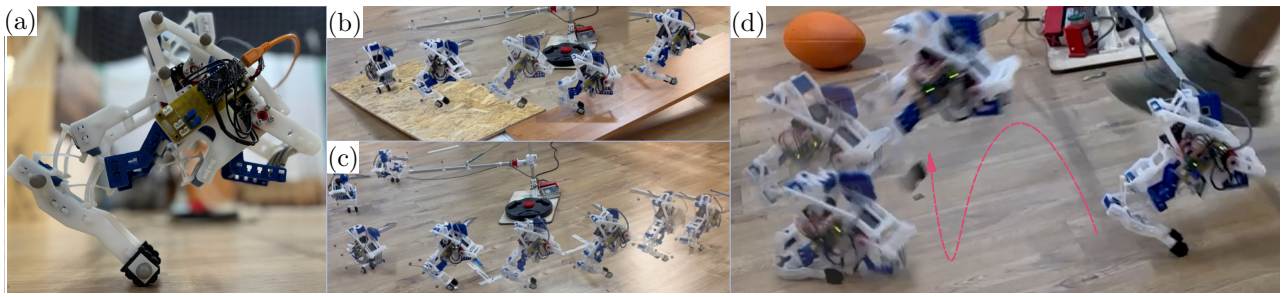

Fig. 5. To validate the proposed co-design method, we constructed a prototype and carried out a series of full-scale experiments: (a) examination of the manufactured leg prototype at rest, (b) testing a ramp jump, (c) forward jumping, and (d) touchdown after a kick

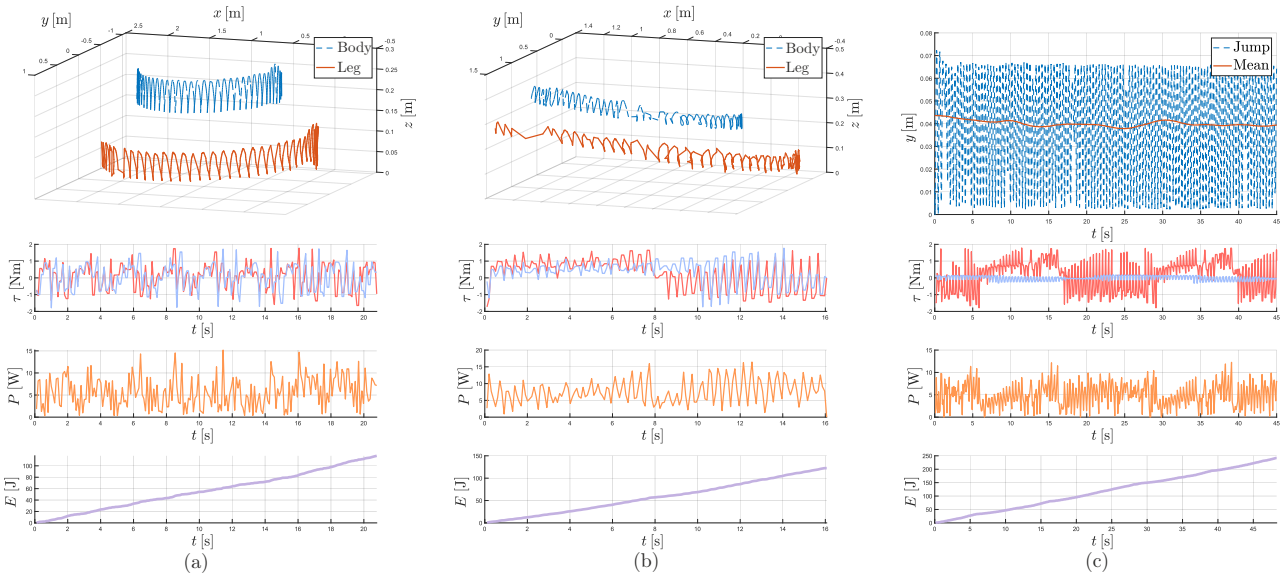

Fig. 6. Experimental data for different locomotion scenarios include: (a) forward jumping, (b) ramp jumping, and (c) jumping in a place. Red and blue lines indicate the torques for the main and mode motors respectively, while orange and violet indicate the energy characteristics

B. Virtual Experiment

We utilized the rotational stiffness and minimum frequency of the compliant mechanism as the outputs of SPACAR simulation model. The springs in Simscape Multibody have been modeled to accurately represent their equilibrium position, stiffness, and damping characteristics.

The DAE solver was used in the simulations, and numerical differentiation tolerances were increased and adjusted to ensure the holonomic constraints converged sufficiently. A penalty-based contact model was employed to simulate the interaction between the foot's toe and the ground. This approach was utilized to accurately capture the behavior of this contact interaction in the simulation.

C. Real Experiment

The physical prototype is attached to a 1.15 meter long rod with a spherical workspace. One side is screwed to the robot and the other side is fixed on the base [20]. Three types of experiments were performed: (1) jumping forward, (2) ramp jumping with a slope of $\beta = 8^\circ$ (3) and jumping in a place (Fig. 5).

TABLE I

DIFFERENT SCENARIOS FEATURES

Scenario	Distance travelled, m	V, m/s	$\tilde{h}$, m	Efficiency
Jumping forward	4.22	0.26	0.045	CoT = 5.3
Ramp jump	4.03	0.24	0.035	CoT = 5.8
Jumping in a place	-	-	0.04	$\tilde{E}$ = 2.1, J

Fig. 6 shows experimental data for different locomotion scenarios include trajectories, torque values, and power consumption. We used *OptiTrack* with 6 cameras to capture the real-time body and leg positions of the robot. The average residual calibration error was 0.36 mm over a ray length of 7.5 m. The operation of the motors was recorded by measuring current and angular position. Torque, velocity, and energy characteristics were calculated based on these parameters. Table I provides a summary of the observed characteristics, where CoT denotes the cost of transport.

Note that the average height in the jumping scenario with the motor running in fixed mode is lower than in the jumping scenario with two motors running synchronously. For the 115 measured jumps in place, the average energy expended per jump is 2.1 J.

IV. Discussion

We conducted an investigation on the integration of three flexure cross hinges (TFCH) into closed-kinematics, shaftless compliant, and impact-robust linkage mechanisms that work under forceful dynamic interaction. A novel parametric optimization procedure for TFCH has been developed and tested for a case study on hopping robot design. It starts from topology, kinematics, and reference trajectory optimization for basic rigid-body closed-kinematics mechanism with further transition to structure with compliant joints and its numeric optimization combining lumped-parameters and finite-element models. The result is the desired TFCH geometry, the optimal joint stiffnesses calculated for that geometry, and the motion frequency supplied as a reference for the motion control system. Field tests demonstrate the high robustness of the prototype to unpredictable external disturbances.

Despite a basic motion planning algorithm and the absence of feedback from the robot to the environment, the robot achieves proficient jumping and is capable of moving with a lateral velocity in the sagittal plane of up to 0.53 m/s. This impressive feat is accomplished with a relatively low cost of transport of 1.3. To realize energy-efficient locomotion, the resonant frequency needs to be calculated considering the mass and stiffness of the robot. Thus, for the payload scenario, we had to calculate the stiffness of CJs.

In the near future, our goal is to create an enhanced control system and a faster, more precise CJ model in order to improve energy efficiency and lower transportation costs, and shrink the reality gap between the simulation model and the physical prototype. Although the current small-size prototype is 100 grams heavier than our previous design with bearings, we expect a better weight ratio for new shaftless design can be achieved with up-scaling. The integration of flexible joints operating in elastic deformation mode provides motion with low intramolecular friction. At the same time, polymers such as nylon have higher viscous deformation characteristics than steel, so this results in higher energy losses. For these reasons, in future research we will focus on developing larger prototypes and utilizing TFCHs made of metal.

References

[1] S. Rezazadeh, A. Abate, R. L. Hatton, and J. W. Hurst, "Robot leg design: A constructive framework," *IEEE Access*, vol. 6, pp. 54 369–54 387, 2018.

[2] K. V. Nasonov, D. V. Ivolga, I. I. Borisov, and S. A. Kolyubin, "Computational design of closed-chain linkages: Hopping robot driven by morphological computation," in *2023 IEEE International Conference on Robotics and Automation (ICRA)*, 2023, pp. 7419–7425.

[3] Y. Ding and U. Thomas, "Improving safety and accuracy of impedance controlled robot manipulators with proximity perception and proactive impact reactions," in *IEEE ICRA*, 2021, pp. 3816–3821.

[4] D. Renjewski, A. Spröwitz, A. Peekema, M. Jones, and J. Hurst, "Exciting engineered passive dynamics in a bipedal robot," *IEEE Transactions on Robotics*, vol. 31, no. 5, pp. 1244–1251, 2015.

[5] J. A. Gallego and J. Herder, "Synthesis methods in compliant mechanisms: An overview," ser. International Design Engineering Technical Conferences and Computers and Information in Engineering Conference, vol. Volume 7: 33rd Mechanisms and Robotics Conference, Parts A and B, 08 2009, pp. 193–214. [Online]. Available: https://doi.org/10.1115/DETC2009-86845

[6] M. Fix, D. Brouwer, and R. Aarts, "Building block based topology synthesis algorithm to optimize the natural frequency in large stroke flexure mechanisms." ASME Digital Collection, Nov. 2020. [Online]. Available: https://event.asme.org/IDETC-CIE-2020, https://event.asme.org/IDETC-CIE

[7] V. Arakelian, "Gravity compensation in robotics," *Advanced Robotics*, vol. 30, no. 2, pp. 79–96, 2016. [Online]. Available: https://doi.org/10.1080/01691864.2015.1090334

[8] W. D. Shin, W. Stewart, M. A. Estrada, A. J. Ijspeert, and D. Floreano, "Elastic-actuation mechanism for repetitive hopping based on power modulation and cyclic trajectory generation," *IEEE Transactions on Robotics*, vol. 39, no. 1, pp. 558–571, 2023.

[9] T. Suzuki, Y. Toshimitsu, Y. Nagamatsu, K. Kawaharazuka, A. Miki, Y. Ribayashi, M. Bando, K. Kojima, Y. Kakiuchi, K. Okada, and M. Inaba, "Ramiel: A parallel-wire driven monopedal robot for high and continuous jumping," in *2022 IEEE/RSJ International Conference on Intelligent Robots and Systems (IROS)*, 2022, pp. 5017–5024.

[10] J. Reher, W.-L. Ma, and A. Ames, "Dynamic walking with compliance on a cassie bipedal robot," *2019 18th European Control Conference (ECC)*, pp. 2589–2595, 2019. [Online]. Available: https://api.semanticscholar.org/CorpusID:131777271

[11] C. W. Mathews and D. J. Braun, "Parallel variable stiffness actuators," in *2021 IEEE/RSJ International Conference on Intelligent Robots and Systems (IROS)*, 2021, pp. 8225–8231.

[12] K. Endo, N. Uchida, R. Morita, and T. Tawara, "Preliminary investigation of powered knee prosthesis with small-scale, light-weight, and affordable series-elastic actuator for walking rehabilitation of a patient with four-limb deficiency," in *2022 International Conference on Robotics and Automation (ICRA)*, 2022, pp. 01–06.

[13] S.-G. Yang, D.-J. Lee, C. Kim, and G.-P. Jung, "A small-scale hopper design using a power spring-based linear actuator," *Biomimetics*, vol. 8, no. 4, 2023. [Online]. Available: https://www.mdpi.com/2313-7673/8/4/339

[14] R. Liang, G. Xu, B. He, M. Li, Z. Teng, and S. Zhang, "Developing of a rigid-compliant finger joint exoskeleton using topology optimization method," in *2021 IEEE International Conference on Robotics and Automation (ICRA)*, 2021, pp. 10 499–10 504.

[15] S. Seltmann and A. Hasse, "Topology optimization of compliant mechanisms with distributed compliance (hinge-free compliant mechanisms) by using stiffness and adaptive volume constraints instead of stress constraints," *Mechanism and Machine Theory*, vol. 180, p. 105133, 2023. [Online]. Available: https://www.sciencedirect.com/science/article/pii/S0094114X22003792

[16] Z. Bons, G. C. Thomas, L. M. Mooney, and E. J. Rouse, "A compact, two-part torsion spring architecture," in *2023 IEEE International Conference on Robotics and Automation (ICRA)*, 2023, pp. 7461–7467.

[17] M. Naves, D. M. Brouwer, and R. G. K. M. Aarts, "Building Block-Based Spatial Topology Synthesis Method for Large-Stroke Flexure Hinges," *Journal of Mechanisms and Robotics*, vol. 9, no. 4, p. 041006, 05 2017. [Online]. Available: https://doi.org/10.1115/1.4036223

[18] B. Okken, J. P. Dekker, J. J. de Jong, and D. M. Brouwer, "Numerical Optimization of Underactuated Flexure-Based Grippers," ser. International Design Engineering Technical Conferences and Computers and Information in Engineering Conference, vol. Volume 8: 47th Mechanisms and Robotics Conference (MR), 08 2023, p. V008T08A041. [Online]. Available: https://doi.org/10.1115/DETC2023-116752

[19] Y. Sim and J. Ramos, "The dynamic effect of mechanical losses of actuators on the equations of motion of legged robots," *ArXiv*, vol. abs/2011.02506, 2020. [Online]. Available: https://api.semanticscholar.org/CorpusID:226254391

[20] J. Ramos, Y. Ding, Y.-W. Sim, K. Murphy, and D. Block, "Hoppy: An open-source kit for education with dynamic legged robots," in *2021 IEEE/RSJ International Conference on Intelligent Robots and Systems (IROS)*, 2021, pp. 4312–4318.